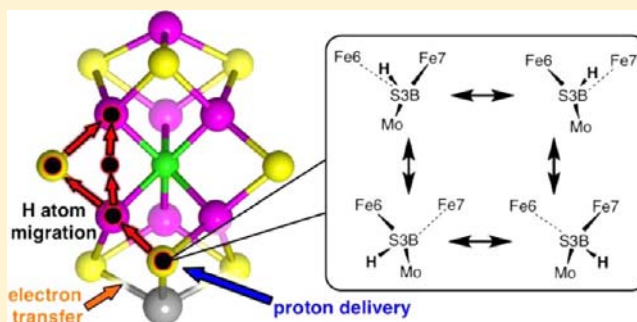


The Stereochemistry and Dynamics of the Introduction of Hydrogen Atoms onto FeMo-co, the Active Site of Nitrogenase

Ian Dance*

School of Chemistry, University of New South Wales, Sydney 2052, Australia

ABSTRACT: The catalyzed hydrogenations effected at the active site FeMo-co of nitrogenase have been proposed to involve serial supply of the required multiple protons along a proton wire terminating at sulfur atom S3B of FeMo-co. In conjunction with serial electron transfer to FeMo-co, these protons become H atoms, and then are able to migrate from S3B to other Fe and S atoms of FeMo-co, and to transfer to bound substrate and intermediates. This general model, which can account for all reactions of nitrogenase, involves a preparatory stage in which each incoming H atom is required to move from the proton delivery side of S3B to the opposite migration side of S3B. This report examines the mechanism of this reconfiguration of S3B-H, finding four stable configurations in which S3B-H has pyramidal-trigonal coordination, with one elongated Fe–S3B interaction. The transition states and energies for reconfiguration are described. Pseudotetrahedral four coordination and planar-trigonal coordination for S3B-H are less stable than pyramidal-trigonal coordination. Results are presented for FeMo-co with one, two, three, and four H atoms (the E₁H₁, E₂H₂, E₃H₃, and E₄H₄ Thorneley–Lowe stages), and the general principles are defined, for application in the various chemical mechanisms of nitrogenase.



INTRODUCTION

Nitrogenase is the enzyme that converts N₂ to NH₃ under mild conditions. While much is known about the processes of this enzyme, the chemical mechanism is still enigmatic.^{1–11} The active site is the iron-molybdenum cofactor, FeMo-co, with the structure shown in Figure 1.^{12–14} The Fe₇MoS₉ cluster contains a central trigonal prismatic set of six Fe atoms, centered by a six-coordinate C atom, and doubly bridged by S atoms on the axial edges. At the top of the cluster, Fe1 is connected through three triply bridging S atoms, and at the bottom, Mo is also connected through three triply bridging S atoms. Four-coordination of Fe1 is completed by cysteine ligation, while six-coordination of Mo is completed with histidine ligation and bidentate chelation by homocitrate.

A series of incisive investigations with modified residues around FeMo-co has identified the Fe2-Fe6 domain of the Fe₂Fe₃Fe₆Fe₇ face of FeMo-co as the site of catalytic reactivity.^{9,15–20} Further, some of these modified proteins allow the trapping of intermediates at low temperature, and the collection of spin-derived^{21–33} and vibrational spectroscopic data.^{34–37} These glimpses of intermediates are very valuable, but still insufficient for the formulation of a detailed chemical mechanism: the conversion of N₂ to 2NH₃ requires at least 15 steps (counted as binding of N₂, collection of six H atoms, formation of six N–H bonds, breaking the N bond, and dissociation of two NH₃ molecules).

In addition to the reaction N₂ + 6H⁺ + 6e⁻ → 2NH₃, there is concomitant reduction of protons, 2H⁺ + 2e⁻ → H₂. Each complete catalytic cycle needs to use about eight protons, and it is clear that these cannot all be provided from the protein

environment surrounding the active site. This immediate environment for substrate and intermediates bound to Fe2/Fe6 is essentially hydrophobic and anhydrous. Instead, there is a chain of hydrogen-bonded water molecules extending from the protein surface to atom S3B of FeMo-co (Figure 2). Detailed analysis of this feature in all crystal structures and species resulted in the recognition of a fully conserved inner section, W8 to W1, which can function as a tightly controlled proton wire.^{38,39} The outer section is variable and probably functions as a proton bay. A standard Grothhuss mechanism can deliver protons serially to S3B in unlimited numbers.³⁹ Alternative suggestions that this path transports substrate⁴⁰ or ammonia³⁸ have been criticized.^{39,41}

It is postulated that proton delivery to S3B is coupled with electron transfer to FeMo-co, effectively generating a H atom bound to S3B. Theoretical simulations have shown how a H atom can migrate from S3B to Fe6, S2B and Fe2.^{42,43} H atoms bound in these positions can then be transferred to contiguously bound substrates and intermediates.^{44–46} As each H atom migrates from S3B to other FeMo-co atoms or to substrate or intermediates, a new proton can be brought to S3B along the proton wire, to become (in conjunction with electronation of FeMo-co) a new H atom on S3B, available for hydrogenation of intermediates.

This cycle of steps introducing H atoms to FeMo-co and its catalytic intermediates is outlined in Scheme 1. This cycle provides a structural description of the generation of the

Received: July 15, 2013

Published: October 29, 2013



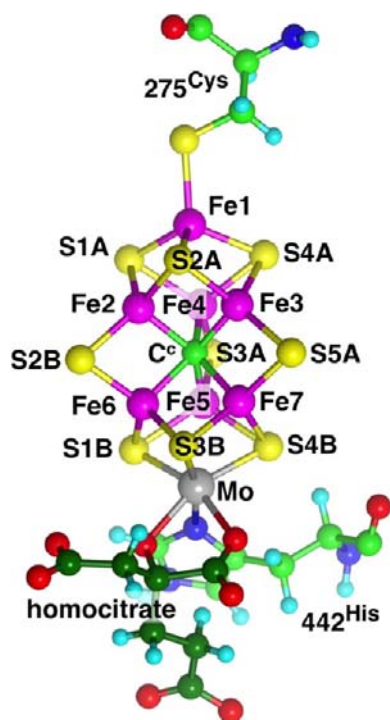


Figure 1. Structure and atom labeling of FeMo-co (*Azotobacter vinelandii*, PDB structure 3U7Q). C atoms of homocitrate are colored dark green.

intermediate states $E_n H_n$, $n = 1, 2, 3, 4 \dots$ in the scheme developed by Thorneley and Lowe to account for their kinetic data on the behavior of nitrogenase.⁴⁷

Each operation of the cycle in Scheme 1 involves a step in which there is inversion of the H atom bound to S3B. This is necessary because the proton supply chain is on the opposite side of S3B to the H atom migration side of S3B. Aspects of this inversion of S3B-H have been described in previous reports, some of which described simulations of FeMo-co with N as central atom, prior to the experimental identification of this atom as C. This paper reports a more comprehensive investigation of the structure-energy surface for the movement of H around S3B, from the receiving side of S3B to the

migratory side of S3B. The simulations are made with C-centered FeMo-co. In addition, an objective here is to develop a deeper understanding of the coordination chemistry of FeMo-co at this end, involving S3B and its bonded atoms Fe6, Fe7, and Mo, as well as roles played by C^c. This is important because the structural chemistry of FeMo-co is affected by the extent and locations of its ligation by H and substrate/intermediates.⁴⁸ Thus, in each of the six circuits of Scheme 1 that must occur in the hydrogenation of N_2 to $2NH_3$, the ligation of FeMo-co will be different, evolving through variable numbers of H atoms, N_2 , N_2H_x intermediates, and NH_x intermediates. The flexible coordination chemistry of the FeMo-co cluster could modify the structure in the vicinity of S3B and thereby modify the inversion dynamics. For reaction cycles with other substrates, such as C_2H_2 , or CO, or D_2 , some of the inversion steps will be different again from those in the N_2 cycle. An understanding of the principles of the coordination of S3B-H and of the inversion dynamics will simplify elucidation of the essential inversion steps.

In earlier papers,^{42,43} the various configurational positions for H around S3B were defined in relation to the bonded atoms Fe6, Fe7, and Mo, as shown in Scheme 2 and labeled with numerals 1–6.

METHODS

Density functional simulations were as previously described,^{42,44,48,49} using DMol3,^{50–52} the blyp functional, numerical basis sets (dnp), unrestricted spins, and fine integration grid. The calculational model of FeMo-co is the same as that used previously, retaining the essential coordination of all atoms: cysteine-275 is truncated to SME, histidine-442 is truncated to imidazole, and homocitrate is truncated to $^-OCH_2COO^-$.⁴⁸ The net charge on this model is -4 , which corresponds to the resting state of FeMo-co.^{53,54} A key component of the calculations is control of the electronic state, because the electronic and spin states of FeMo-co are numerous and energetically close. Electronic states of FeMo-co and derivatives are characterized by the set of signed spin densities on the metal atoms: while the combinations of signs of the metal spins are usually sufficient to characterize an electronic state, there are sometimes different states with the same sign set, but different magnitudes. The total spin S of an FeMo-co derivative is defined in the usual way.

The procedures used to control electronic states have been described, as have the general characteristics of the more stable electronic states.⁵⁵ My investigations of FeMo-co derivatives involve

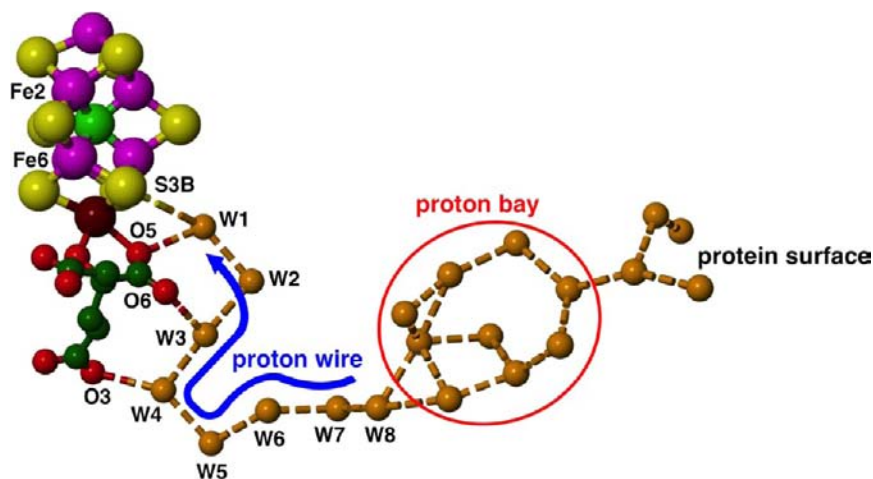
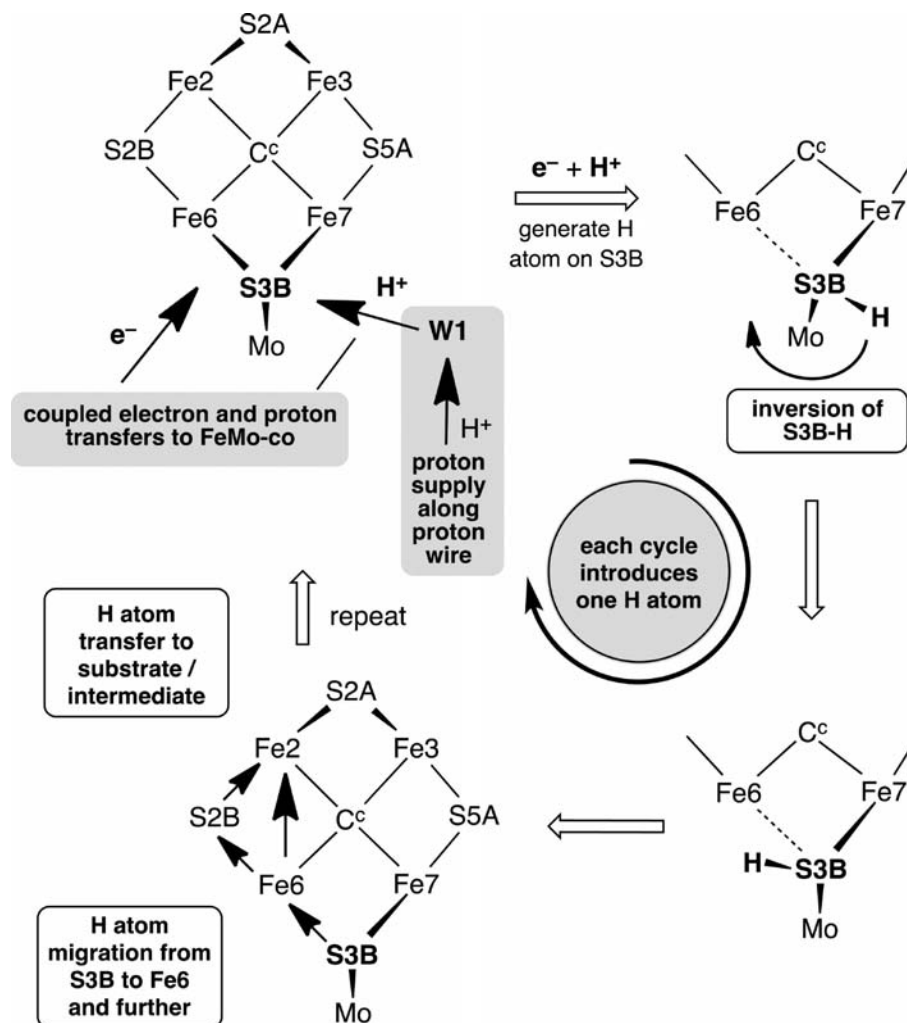


Figure 2. Water path and proposed proton wire (W8 to W1) for delivery of protons by a Grotthuss mechanism from the proton bay to S3B of FeMo-co (Mo is brown).

Scheme 1. General Cycle for (1) Generation of a H Atom on S3B (Using a Proton from the Proton Wire and an Electron Generated in the Fe-Protein Cycle of Nitrogenase), (2) Inversion of H around S3B, and (3) Migration of H from S3B to Other Atoms of FeMo-co and/or Substrates



Scheme 2. The Numbering of Positions for H around S3B

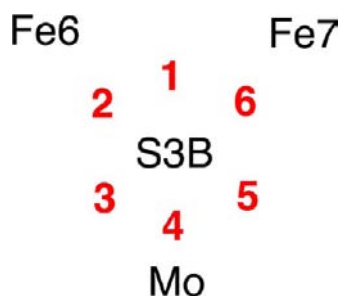


Table 1. Metal Spin Sets (Sign Combinations) and Their Identifying Labels Used in This Work To Describe Electronic States (All Are S Positive)

	A	B	D	F
Fe1	+	+	+	+
Fe2	-	-	-	+
Fe3	+	-	+	-
Fe4	-	+	-	-
Fe5	+	-	+	+
Fe6	+	+	-	-
Fe7	-	+	-	+

initial explorations of possible spin sets and total spins, informed by the general principles for stability of electronic states, in order to then focus on the most stable electronic/S states. I use letter labels to identify the various combinations of signs of the Fe spin densities: those labels relevant to this paper are defined in Table 1. In the results described below the electronic state is labeled as X(S), where X is the letter for the sign combination, and S (0, 1/2, 1, etc.) is the total spin.

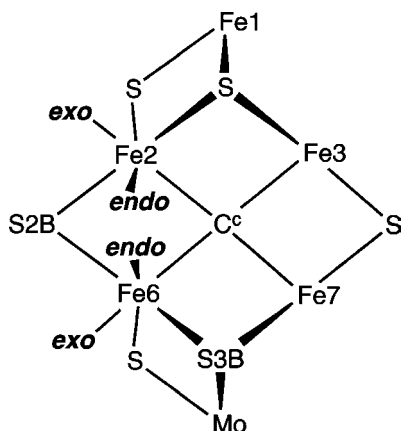
Transition states were determined by the procedure previously described.^{56,57} This method, which allows general exploration of the geometry-energy surface, is valuable where the reaction coordinate involves a number of geometrical changes. In the trans-configurations occurring in the systems described here, there can be changes in S3B–

Fe, S3B–Mo, and C^c–Fe distances as well as movement of the H atom. Further description and discussion of the method is provided at a relevant point in the results below.

RESULTS

Results are presented for FeMo-co bearing one, two, three, and four H atoms. The labeling system used for hydrogenated forms of FeMo-co is $nH.ww.xx.yy.zz$, where n is the number of introduced H atoms, and the codes ww , xx , etc. describe the locations of those H atoms. The location codes are $2x$, $2n$, $6x$, $6n$ for the *exo* and *endo* coordination positions (see Scheme 3)

Scheme 3



on Fe2 and Fe6, respectively, 26 for H bridging Fe2 and Fe6, 2b for H on S2B, and 3b for H on S3B. The convention is to list Fe-bound locations of H atoms before S2B, S3B locations.

The First H atom on S3B of FeMo-co. The first intermediate examined was **1H.3b**, which has one H atom bound in various ways to S3B. Of the six feasible configurations (Scheme 2), four are energy minima, and two of them, **1** and **4**, are transition states between the contiguous configurations. The four stable configurations are labeled **3b2**, **3b3**, **3b5**, and **3b6**. The essential structures and structural relationships between these four configurations are shown in Figure 3, together with four relevant transition states connecting the configurational minima.

In each of the four configurations for **1H.3b**, one of the S3B–Fe bonds is normal, while the other is elongated to the extent of being nonexistent. These long interactions are marked as broken lines in Figure 3. In each of the stable configurations, the coordination number of S3B is 3 (Mo,Fe,H), and its

stereochemistry is trigonal-pyramidal. This is a general characteristic of S3B bearing a H atom. Further, on each of the edges of the square array in Figure 3, each transition between contiguous configurations of S3B–H involves an interchange of the normal and the elongated Fe–S3B interactions. To illustrate, **3b5** with normal Fe7–S3B and elongated Fe6–S3B becomes **3b3** with elongated Fe7–S3B and normal Fe6–S3B. Concomitant with this, all four of the transition states on the edges of Figure 3 involve S3B–H with two approximately equivalent connections to Fe, and loose 4-fold coordination (Mo,Fe6,Fe7,H).

Details of these geometries and geometrical changes are portrayed (for electronic state D(0)) in Figure 4, which shows only the immediately involved atoms: the central C^cFe₆ core and remainder of FeMo-co are essentially unchanged and are not shown. The trigonal-pyramidal coordination of S3B–H in each of the four stable configurations is clearly evident. Table 2 contains the interatomic distances required for more incisive interpretation. The Mo–S3B distance is essentially invariant (ca. 2.53 Å), as is the normal Fe–S3B bond (ca. 2.39 Å) in each of the four configurations. The elongated Fe–S3B, which permits the trigonal coordination of S3B–H, ranges from 2.75 to 2.98 Å: a consequence of this is that one Fe is under-coordinated in each of the four configurations. Mo–H distances are nonbonding.

Only one of the four transition states (TS 5-3) has approximate tetrahedral stereochemistry at S3B. TS 3-2 and TS 5-6 have irregular stereochemistry at S3B, with two equal, but lengthened, Fe–S3B bonds, while TS 6-2 is more unusual with irregular stereochemistry and longer (ca. 2.73 Å) Fe–S3B distances.

The potential energy changes (kcal mol⁻¹) through each of the transition states are marked in Figure 4. On the energy surface for the D(0) electronic state, the four stable configurations are effectively equi-energetic (within 2 kcal

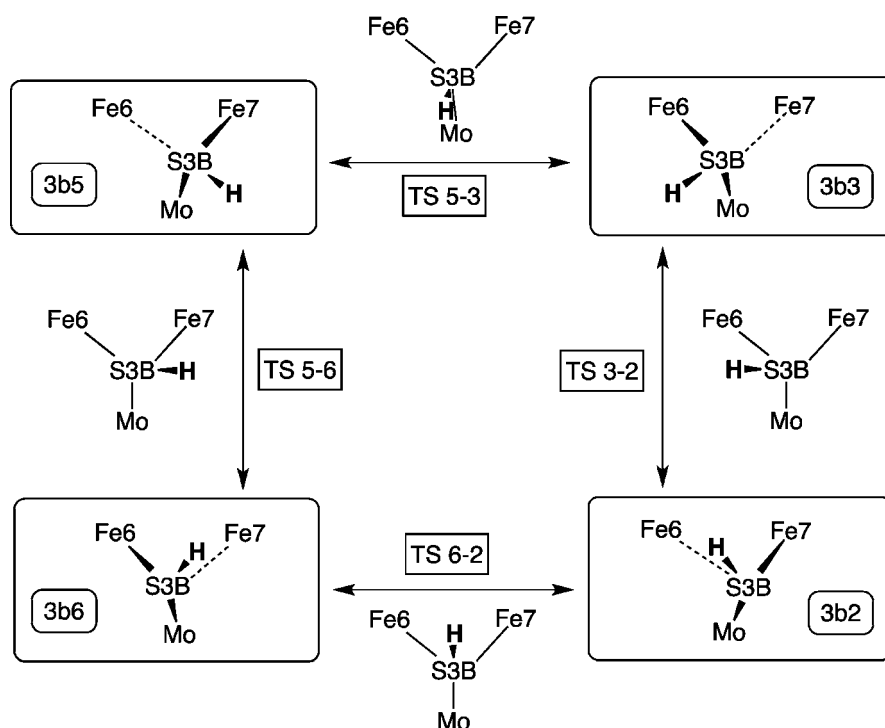


Figure 3. Configurations and transition states (TSs) for **1H.3b**. Elongated bonds are drawn as broken lines.

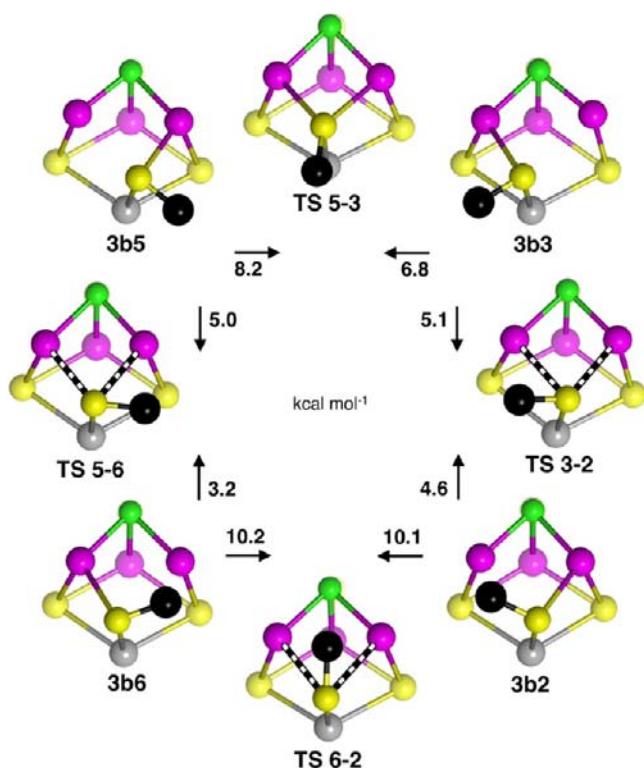


Figure 4. Geometrical structures for the four configurations of H on S3B of FeMo-co (**1H.3b**), and the four transition states. The remainder of FeMo-co is essentially invariant geometrically and is not shown. The electronic state of all species is D(0). H (black) is exaggerated in size; Mo is gray. The energy steps to the transition states are marked, in kcal mol⁻¹. The black/white striped Fe–S3B bonds are elongated.

Table 2. Relevant Interatomic Distances (Å) for the Stable Configurations and Transition States of S3B-H, in Electronic State D(0)

	S3B–Fe6	S3B–Fe7	S3B–Mo
3b5	2.88	2.37	2.50
TD 5-3	2.37	2.47	2.52
3b3	2.37	2.98	2.52
TS 3-2	2.57	2.55	2.54
3b2	2.75	2.41	2.54
TS 6-2	2.71	2.74	2.57
3b6	2.39	2.76	2.54
TS 5-6	2.55	2.56	2.53

mol⁻¹), and the barriers between them are energetically symmetrical. For the general hydrogenation mechanism of nitrogenase action (Scheme 1), the required progress is from configuration **3b5** to configuration **3b2**. Configuration **3b5** has S3B displaced toward the water molecule at the end of the proton wire, while configuration **3b2** has the H on S3B directed toward Fe6, ready for H migratory steps. Mechanistic reconfiguration from **3b5** to **3b2** could use either the pathway via **3b3** or the pathway through **3b6**, with the **3b3** path having slightly lower barriers.

What about direct reconfiguration from **3b5** to **3b2**, across the diagonal of Figure 3? This involves inversion through an Fe7MoS3B-H geometry, which is planar at S3B, and calculations indicate that the energy of this transition state is ca. 10 kcal mol⁻¹ higher than any of the nonplanar transition

states of Figure 4. For this reason, the direct route from **3b5** to **3b2** has not been evaluated further.

For the different electronic/spin state B(1) of **1H.3b**, the four configurations and their interconversions are essentially the same as those already described for the D(0) state. Figure 5 shows the energies to the four transition states, and the Fe6–S3B and Fe7–S3B distances as the main geometric variables. The interconversion barriers are roughly 1 kcal mol⁻¹ larger than those for state D(0).

It could be expected that the variable coordination of Fe6 and Fe7 in the four configurations of **1H.3b** would be reflected as variations in their spin densities. Table 3 contains the calculated spins for the Fe and Mo atoms in the four configurations and four transition states in the D(0) electronic state: there is but minor variation in the spins. The spin densities for S3B and H in these structures are close to zero. Similar minor variation in the metal spins across the configurational changes occur in electronic state B(1).

The A(1) electronic state for the configurations of **1H.3b** is more complex. Configuration **3b2** exists in two different A(1) states, one with normal small spin magnitude (<0.5) at Mo, whereas the other has large spin on Mo. Configuration **3b5** has small Mo spin, whereas configurations **3b3** and **3b6** have large Mo spin. Details are contained in Table 4, together with the relative energies of the configurations and transition states. In the reconfigurations **3b5** → TS 5-3 → **3b3** and **3b6** → TS 6-2 → **3b2**, there are large changes in the magnitude of the Mo spin, and it has been confirmed that these are continuous changes and not jumps between different electronic states. The geometry of the **3b2** configuration (large Mo spin) that arises by reconfiguration from **3b3** is different, in that the Fe6–S3B distance (2.56 Å) is not as elongated as in other states (ca. 3 Å), and the H atom is almost bridging between S3B and Fe6. This structure is also 2–3 kcal mol⁻¹ less stable than normal. The reconfigurational potential energy barriers for electronic state A(1) are comparable with those of the D(0) and B(1) electronic states.

Configurations of 2H.2b.3b. After migration of the first H atom from S3B to other atoms of FeMo-co, a second H atom can be introduced to S3B. When the second H atom is bound to S3B, the first H atom could be in any of six possible bonded positions, namely, *exo*-Fe6, *endo*-Fe6, bridging Fe6 and Fe2, S2B, *endo*-Fe2, or *exo*-Fe2. Of these, the S2B-H structure is at least 5 kcal mol⁻¹ more stable than any of the others,⁵⁸ and therefore, the S3B-H configurations for the second H were investigated with the first H bound to S2B, that is intermediate **2H.2b.3b**. In these structures, all of the bonds between C^c and the surrounding six Fe atoms are normal at ca. 2 Å, as in **1H.3b**, and calculations encompassing several electronic states indicate that the interconfigurational transformations are geometrically and electronically similar to those of **1H.3b**.

Configurations of 3H.2x.2b.3b. The S3B-H configurations for the third H added to FeMo-co were investigated for intermediate **3H.2x.2b.3b** in which the first two H atoms are bound to S2B and *exo*-Fe2. This intermediate was selected here for two reasons: first, because this is among the more stable of the structures with this number of H atoms and, second, because it introduces the C^c–Fe2 interaction (distance) as a variable. The four configurational minima (for electronic state D(0)) are pictured in Figure 6. The coordination at Fe2 is approximately trigonal-bipyramidal, and the Fe2–C^c distance is elongated from 2.0 to 2.4–2.5 Å. This extension of one Fe–C^c interaction is common in many forms of FeMo-co in which H,

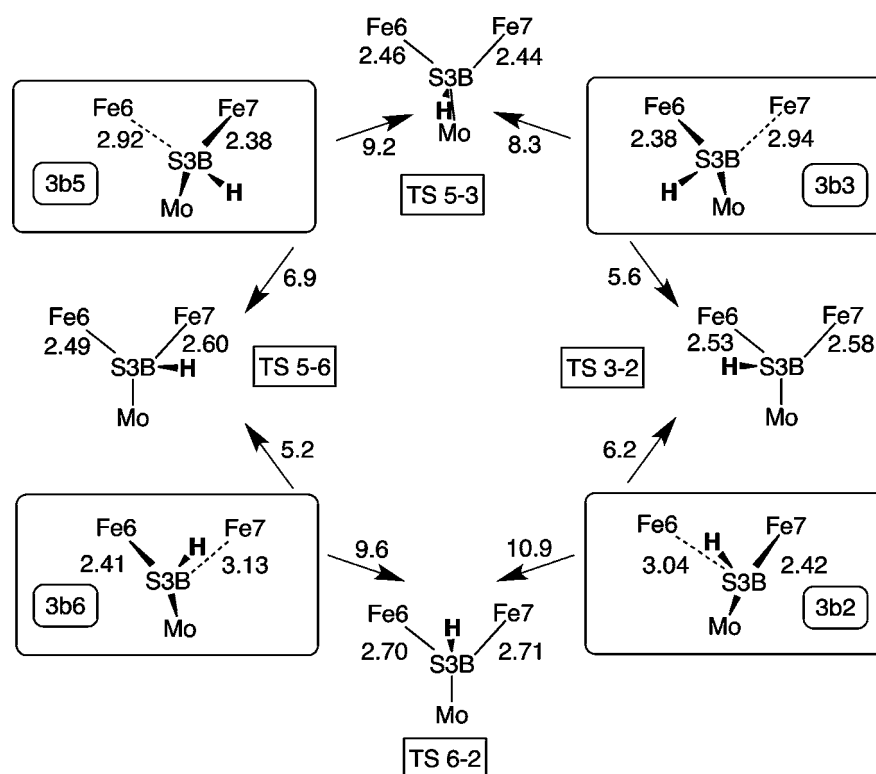


Figure 5. Properties of the array of stable configurations and transition states for **1H.3b** in electronic state B(1). Values on the arrows are the energy differences (kcal mol^{-1}) comparable with those in Figure 4. The Fe6–S3B and Fe7–S3B distances (Å) are marked.

Table 3. Calculated Spin Densities for the Fe and Mo Atoms of the Configurations and Transition States of **1H.3b** in Electronic State D(0)^a

	3b5	TS 5-3	3b3	TS 3-2	3b2	TS 6-2	3b6	TS 6-5
Fe1	3.12	3.06	3.11	3.12	3.08	3.08	3.09	3.10
Fe2	-2.83	-2.24	-2.41	-2.22	-1.94	-1.87	-1.91	-2.06
Fe3	2.94	2.96	3.05	3.07	3.03	3.03	3.06	3.05
Fe4	-2.82	-2.64	-2.68	-2.62	-2.45	-2.58	-2.57	-2.55
Fe5	2.33	2.70	2.31	2.34	2.41	2.17	2.26	2.34
Fe6	-0.61	-1.99	-2.01	-2.05	-2.29	-2.08	-1.98	-2.14
Fe7	-2.42	-2.23	-2.30	-2.53	-2.37	-2.48	-2.50	-2.43
Mo	0.15	0.21	0.61	0.57	0.21	0.45	0.28	0.35

^aSpin densities for the other atoms not listed complete the total $S = 0$.

Table 4. Calculated Spin Densities and Relative Energies for the Configurations and Transition States of **1H.3b** in Electronic State A(1)^a

	3b5	TS 5-3	3b3	TS 3-2	3b2 from TS 3-2	3b2 from TS 6-2	TS 6-2	3b6
Fe1	3.15	3.15	3.15	3.15	3.14	3.15	3.14	3.16
Fe2	-2.77	-2.85	-2.79	-2.78	-2.77	-2.78	-2.82	-2.80
Fe3	2.98	2.89	2.96	2.95	2.95	2.96	2.91	2.91
Fe4	-2.77	-2.81	-2.79	-2.77	-2.76	-2.77	-2.79	-2.80
Fe5	2.37	2.49	2.57	2.64	2.66	2.37	2.44	2.61
Fe6	1.78	2.17	2.79	2.64	2.61	1.90	2.26	2.69
Fe7	-2.58	-2.67	-2.68	-2.74	-2.73	-2.61	-2.75	-2.61
Mo	-0.24	-0.44	-1.67	-1.42	-1.42	-0.29	-0.45	-1.56
relative energy kcal mol^{-1}	0.0	8.9	0.7	4.0	3.0	0.9	10.8	0.9

^aSpin densities for the other atoms not listed complete the total $S = 1$.

substrates, or intermediates are coordinated in the *exo*-Fe position.^{44,46,48,54}

The S3B-H configurations for **3H.2x.2b.3b** in Figure 6 (for electronic state D(0)) are essentially the same as those for

1H.3b, with similarly elongated Fe–S3B distances enabling the trigonal coordination of S3B-H, and the four configurations are approximately equi-ergonic. Relative energies are: **3b5** 0.8, **3b3** 0.1, **3b6** 0, and **3b2** 1.7 kcal mol^{-1} . Energy barriers (kcal mol^{-1})

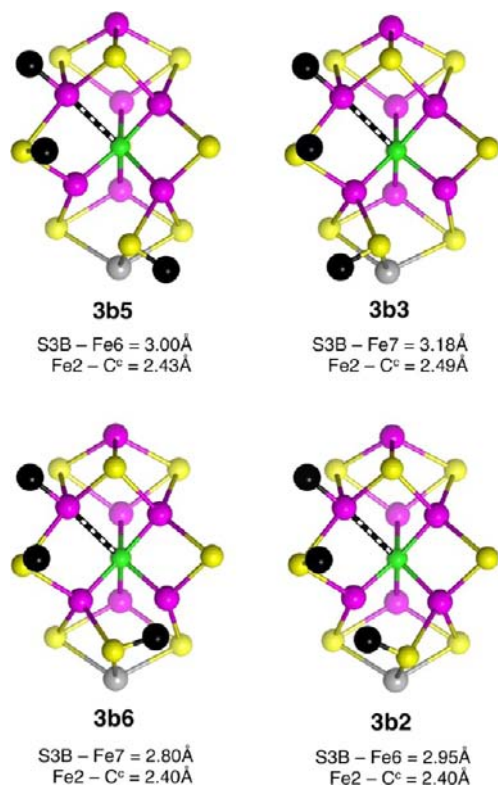


Figure 6. Structures for the configurations of 3H.2x.2b.3b, in electronic state D(0).

for reconfigurations are: 3b5 +6.2 → TS 5-3 –7.0 → 3b3; 3b5 +1.8 → TS 5-6 –2.6 → 3b6; 3b6 +9.3 → TS 6-2 –7.7 → 3b2.

Introduction of the Fourth H Atom. After migration of the third H atom to FeMo-co, there are at least eight different structural possibilities with these H atoms bound to Fe2 and/or S2B and/or Fe6. Of these, the most stable have the H atoms distributed as in 3H.6x.26.2b and 3H.2x.6x.2b. These intermediates have a H atom in the *exo* position of Fe6, an attribute that is expected to influence the configurations of H on the adjacent S3B and the reconfiguration steps. Investigation of these configurations and their interchanges focused on structure 3H.2x.6x.2b, because, in possessing *exo*-Fe2-H and having the *endo* position of Fe6 vacant, it is relevant to the proposed mechanism for complete hydrogenation of N₂^{44,54} and other substrates.^{43,46,58}

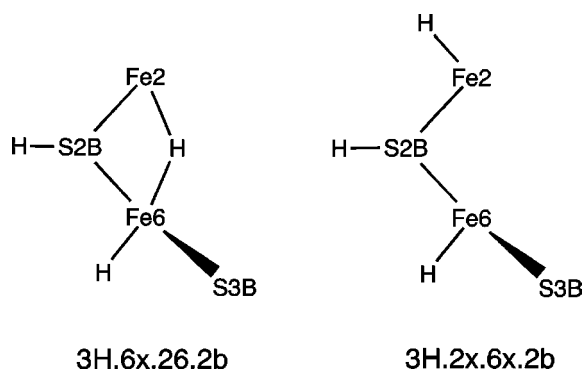


Figure 7. Structures for the configurations of 4H.2x.6x.2b.3b, in electronic state D(1/2). The a/b isomers reflect C^c–Fe distance variations, as marked (Å). Additional distances are S3B–Fe7 = 2.60 Å in 3b6, S3B–Fe6 = 3.71 Å in 3b2-a, and S3B–Fe6 = 3.78 Å in 3b2-b.

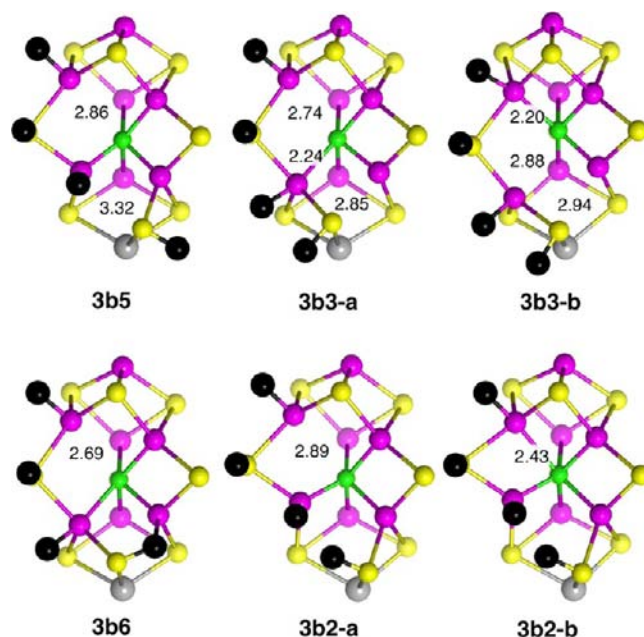


Figure 7. Configurations of H-S3B for intermediate 4H.2x.6x.2b.3b, in electronic state D(1/2). The a/b isomers reflect C^c–Fe distance variations, as marked (Å). Additional distances are S3B–Fe7 = 2.60 Å in 3b6, S3B–Fe6 = 3.71 Å in 3b2-a, and S3B–Fe6 = 3.78 Å in 3b2-b.

and 3b2, there are geometrical isomers arising in variations of the Fe–C^c distances. For all four configurations, there is a structure with the Fe2–H entity distant from C^c, such that Fe2 attains standard tetrahedral coordination, whereas, in the isomers 3b2-b and 3b3-b, there is five-coordination of Fe2. The coordination stereochemistry at Fe6 is approximately tetrahedral in 3b5, 3b2-a, and 3b2-b due to a bending of H–Fe6 toward the distant S3B. Notice that, in configuration 3b2, the H atoms on Fe6 and S3B are directed toward each other, at a H–H separation of 1.94 Å (3b2-a) or 1.89 Å (3b2-b): the formation of H₂ from intermediate 4H.2x.6x.2b.3b2 will be described separately in an account of the complete hydrogen chemistry of FeMo-co.⁵⁸ In 3b3, the distance between H on Fe6 and H on S3B is 2.46 Å (3b3-a) or 2.51 Å (3b3-b). Configuration 3b6 is unusual because the H atom bridges the shorter (2.60 Å) gap between S3B and Fe7, with H–S3B = 1.42 Å, H–Fe7 = 1.98 Å. This bridging geometry for 4H.2x.6x.2b.3b6 occurs in electronic states A(3/2) and F(3/2) as well as D(1/2).

The geometric abnormalities in the configurations of 4H.2x.6x.2b.3b are reflected in their relative energies, which are 3b5 +0.4, 3b3-a +11.6, 3b3-b +9.6, 3b6 +6.1, 3b2-a +0.7, and 3b2-b 0 kcal mol⁻¹ in electronic state D(1/2). The energy dispersion of the configurations of 4H.2x.6x.2b.3b differentiates it from intermediates 1H.3b, 2H.2b.3b and 3H.2x.2b.3b in which the configurations are close to equi-energetic. The main factor in the 4H.2x.6x.2b.3b configurations is extra stability for 3b5 and 3b2 that arises from the bending of H–Fe6 and achievement of favorable coordination stereochemistry at Fe6. This source of stabilization is evident in the course of optimization of these structures.

The calculated spins for Fe and Mo in the configurations of 4H.2x.6x.2b.3b (D(1/2)) are normal, with consistently small values for Mo. The spins for Fe2 and Fe6, both ligated by H, are characteristically smaller in magnitude than those of the other Fe atoms. Concomitant with this, there are relatively

small differences between the spin magnitudes for geometrical isomers **3b2-a** and **3b2-b**, and between **3b3-a** and **3b3-b**.

The configurational interchange steps for **4H.2x.6x.2b.3b** are partly complicated by the occurrence of Fe–C⁺ isomers, and by the unusual structure of **3b6**. Figure 8 shows the structures of

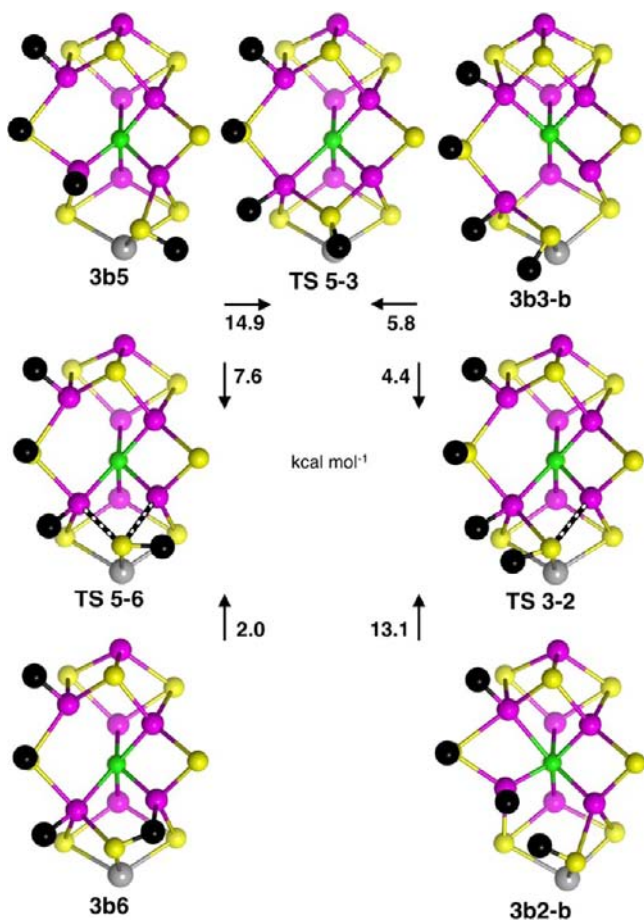


Figure 8. Reconfiguration transition states and energies (kcal mol⁻¹) for **4H.2x.6x.2b.3b**, electronic state D(1/2).

calculated transition states for the **3b5** → **3b3**, **3b5** → **3b6**, and **3b3** → **3b2** reconfigurations, and the energies for crossing these barriers. The unusually large barrier of 14.9 kcal mol⁻¹ for the **3b5** → **3b3** step is due to the above-mentioned additional stability of **3b5**.

Not shown in Figure 8 is the configurational interchange between **3b6** and **3b2**. This domain of configurational space is more complicated, because it overlaps with the migration of H from S3B to an Fe atom. The behavior can be demonstrated by the outcomes of some key calculations that were undertaken to determine transition state. The pragmatic method used to find the saddle point on the potential surface between two local energy minima involves an iterative sequence of partial energy reduction calculations, each of which uses atom displacement steps that are very small (usually 0.025 Å). These small-step small-extent energy reductions proceed from trial structures that must oscillate across the energy barrier, and bracket the saddle point with diminishing excursions from it. To illustrate this procedure, a first trial (guessed) geometry between reactant and product is energy-minimized until the direction of geometry change is clear. From this, a second trial on the other side of the barrier can be estimated, and its energy

reduction course and energy gradients are monitored: a point with a relatively low energy gradient is selected, and from this, the key atoms are moved to the geometry just back across the barrier. Iteration of this process, necessarily oscillating across the barrier, and with diminishing distances between trial structures, converges the geometry toward the saddle point. The saddle point is confirmed by the energy gradients that approach zero, and by optimization to reactant or product when the geometry is nudged slightly. This method works because all variables that are conjugate to the reaction coordinate are automatically optimized through the sequence of energy reductions. This method is particularly effective for FeMo-co reaction systems, such as those described in this report, where many atoms are moving.

Application of this method to the space between configurations **3b6** and **3b2** of **4H.2x.6x.2b.3b** in electronic state D(1/2) yielded results shown in Figure 9. The three structures A, B, and C very close to saddle points are almost identical in energy (within 0.1 kcal mol⁻¹) and are very similar in geometry, and have low energy gradients, but on energy minimization lead to three different stable structures. One of

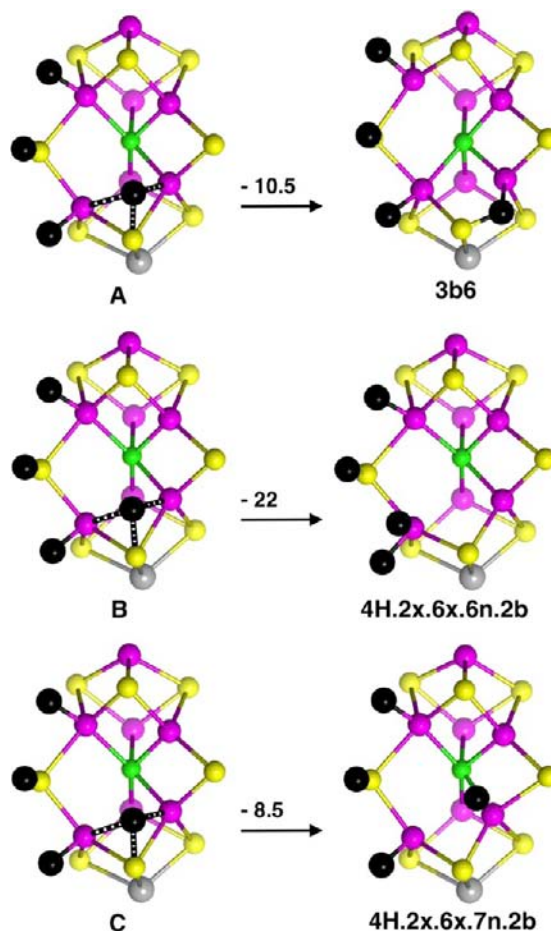
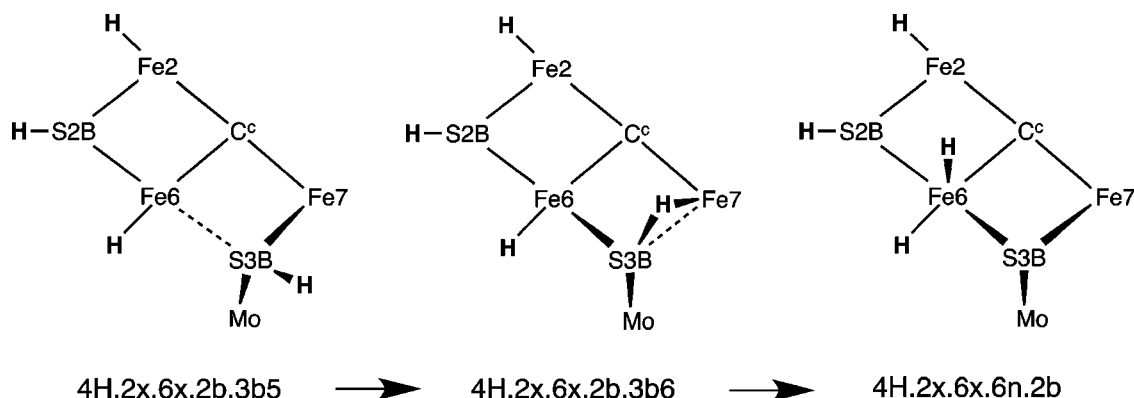


Figure 9. Closely related equi-energetic structures A, B, and C demonstrating a saddle domain on the potential energy surface connecting configuration **3b6** to products **4H.2x.6x.6n.2b** and **4H.2x.6x.7n.2b**, in electronic state D(1/2). The energy reductions marked are in kcal mol⁻¹. Interatomic distances (Å) for A, B, C, respectively, are H–S3B 1.50, 1.54, 1.52; H–Fe6 2.21, 2.07, 2.12; H–Fe7 1.80, 1.80, 1.78; S3B–Fe6 2.33, 2.31, 2.30; S3B–Fe7 2.50, 2.48, 2.46; S3B–Mo 2.48, 2.46, 2.46.

Scheme 4



these is configuration **3b6**, but configuration **3b2** is not connected to this A/B/C near transition state. The potential energy surface in the vicinity of A/B/C involves an elongated S3B–H interaction (1.52 Å, normally 1.37 Å), and because S3B is close to both Fe6 (2.31 Å) and Fe7 (2.49 Å), the energy valleys from A/B/C involve H atom migration to the *endo* positions of either Fe6 (structure **4H.2x.6x.6n.2b**) or Fe7 (structure **4H.2x.6x.7n.2b**) (Figure 9). The relevant interatomic distances demonstrating the similarity of A, B, and C are given in the caption to Figure 9. Further precise calculations would be able to locate distinct saddle points between **3b6** and the two possible products, but there is little reason to do this because direct pathways from H on S3B to H on Fe of FeMo-co are now evident. In effect, the separate steps involving reconfiguration of H on S3B, followed by H migration to Fe, have merged into a single step (Scheme 4). The essential reason for this unconventional behavior is the tight geometry of the Fe6–S3B–H–Fe7 domain of **4H.2x.6x.2b.3b6**.

The pathway of most interest for the fourth H atom adding to S3B when three prior H atoms are bound at S2B, *exo*-Fe2, and *exo*-Fe6 involves the starting configuration **4H.2x.6x.2b.3b5**, moving through TS 5-6 to **4H.2x.6x.2b.3b6** with a barrier of 7.6 kcal mol⁻¹ (Figure 8), and then moving to **4H.2x.6x.6n.2b** with a barrier of ca. 10.5 kcal mol⁻¹. Also, because these steps are intramolecular, and the H atom is moving short distances, it is highly likely that quantum H tunneling occurs here, effectively diminishing these classical potential energy barriers.^{45,59}

DISCUSSION

The proposed model for all of the hydrogenation reactions of nitrogenase involves a serial stream of protons delivered from the end of the proton wire to S3B (made more basic by electron transfer to FeMo-co), where they become nascent H atoms bound to S3B. Each such H atom moves from the delivery side of S3B to the migratory side of S3B, and then to the substrate. This is a repeated fundamental process in the proposed model. This investigation has established that the reconfiguration of H from one side of S3B (**3b5**) to the opposite side (**3b2**) is most generally a two-stage process, passing through intermediate configurations (**3b3**, **3b6**) in which H moves around S3B rather than over it. Direct inversion of S3B–H, which would require a transition state with planar S3B coordination, is energetically less favorable than passage through intermediates and transition states that have elongated S3B–Fe interactions.

In this context, some principles for the coordination chemistry of S3B–H are evident. Pyramidal-trigonal coordination of S3B is more stable than planar-trigonal coordination. Elongation of one Fe–S3B(H) bond (from ca. 2.4 to ca. 3 Å), a requirement for trigonal coordination of S3B–H, involves no energy penalty, even through there is concomitant diminution of the coordination of the Fe atom. This reduced coordination of an Fe6 or Fe7 atom, caused by S3B–H, is linked to the coordination of the Fe atom by C^c. In all structures, an Fe atom that has an elongated weak Fe–S3B–H interaction does not have an elongated Fe–C^c interaction, and in a number of cases, that Fe–C^c distance is shorter than the usual 2.04 Å. Geometrical isomers involving elongation of one Fe–C^c distance are calculated to be feasible and probably important in the coordination chemistry of derivatives and reaction steps of FeMo-co,^{48,54} and are evident here in Figures 6–8. However, in each preparatory stage introducing a new H atom, with reconfiguration of S3B–H, an Fe6 or Fe7 atom would *not* have elongated bonds with *both* C^c and S3B.

The coordination number of S3B deserves further comment. The S3B atom of FeMo-co is usually triply bridging, with two S3B–Fe distances ca. 2.3 Å and Mo–S3B ca. 2.4 Å. However, in the energy minima calculated here for hydrogenated S3B, at least one of these distances is longer. The transition states TS 5-3 have some lengthening of all three bonds to S3B, and the transition structure A/B/C has elongation of S3B–H in addition to some lengthening of S3B–Fe7 and S3B–Mo. There is no indication here that four-coordinate (pseudotetrahedral) S3B is stable. This observation is supported by interrogation of the Cambridge Structural Database⁶⁰ for molecules containing the entities (μ₃-SH)M₃ and (μ-SH)M₂. There six crystal structures for four chemical systems classified as containing (μ₃-SH)M₃, but in none of these is this structure characterized unambiguously.^{61–63} In contrast, there are many instances of (μ-SH)M₂ with pyramidal stereochemistry. Kuwata and Hidai reached the same conclusion about the scarcity or nonexistence of (μ₃-SH)M₃ in their review of M-SH complexes.⁶⁴

This preference for SH bridging two metals is consistent with the intuitive principle that doubly bridging S would be more Bronsted basic than triply bridging S. Indeed, this concept is implicit in the conformation **3b5** in which doubly bridging S3B first abstracts a proton from the terminus of the proton wire.

AUTHOR INFORMATION

Corresponding Author

*E-mail: i.dance@unsw.edu.au.

Notes

The authors declare no competing financial interest.

ACKNOWLEDGMENTS

This research was supported by the University of New South Wales and was undertaken on the NCI National Facility in Canberra, Australia, which is supported by the Australian Commonwealth Government.

REFERENCES

- (1) Burgess, B. K.; Lowe, D. J. *Chem. Rev.* **1996**, *96*, 2983.
- (2) Howard, J. B.; Rees, D. C. *Chem. Rev.* **1996**, *96*, 2965.
- (3) Rees, D. C.; Howard, J. B. *Curr. Opin. Chem. Biol.* **2000**, *4*, 559.
- (4) Christiansen, J.; Dean, D. R.; Seefeldt, L. C. *Annu. Rev. Plant Physiol. Plant Mol. Biol.* **2001**, *52*, 269.
- (5) Igarashi, R. Y.; Seefeldt, L. C. *Crit. Rev. Biochem. Mol. Biol.* **2003**, *38*, 351.
- (6) Rees, D. C.; Tezcan, F. A.; Haynes, C. A.; Walton, M. Y.; Andrade, S.; Einsle, O.; Howard, J. A. *Philos. Trans. R. Soc., A* **2005**, *363*, 971.
- (7) Howard, J. B.; Rees, D. C. *Proc. Natl. Acad. Sci. U.S.A.* **2006**, *103*, 17119.
- (8) Peters, J. W.; Szilagyi, R. K. *Curr. Opin. Chem. Biol.* **2006**, *10*, 101.
- (9) Seefeldt, L. C.; Hoffman, B. M.; Dean, D. R. *Annu. Rev. Biochem.* **2009**, *78*, 701.
- (10) Yang, Z.-Y.; Danyal, K.; Seefeldt, L. C. *Methods Mol. Biol.* **2011**, *766*, 9.
- (11) Hu, Y.; Lee, C. C.; Ribbe, M. W. *Dalton Trans.* **2012**, *41*, 1118.
- (12) Einsle, O.; Tezcan, F. A.; Andrade, S. L. A.; Schmid, B.; Yoshida, M.; Howard, J. B.; Rees, D. C. *Science* **2002**, *297*, 1696.
- (13) Spatzal, T.; Aksoyoglu, M.; Zhang, L.; Andrade, S. L. A.; Schleicher, E.; Weber, S.; Rees, D. C.; Einsle, O. *Science* **2011**, *334*, 940.
- (14) Lancaster, K. M.; Roemelt, M.; Ettenhuber, P.; Hu, Y.; Ribbe, M. W.; Neese, F.; Bergmann, U.; DeBeer, S. *Science* **2011**, *334*, 974.
- (15) Barney, B. M.; Igarashi, R. Y.; Dos Santos, P. C.; Dean, D. R.; Seefeldt, L. C. *J. Biol. Chem.* **2004**, *279*, 53621.
- (16) Seefeldt, L. C.; Dance, I. G.; Dean, D. R. *Biochemistry* **2004**, *43*, 1401.
- (17) Dos Santos, P. C.; Igarashi, R.; Lee, H.-I.; Hoffman, B. M.; Seefeldt, L. C.; Dean, D. R. *Acc. Chem. Res.* **2005**, *38*, 208.
- (18) Dos Santos, P. C.; Mayer, S. M.; Barney, B. M.; Seefeldt, L. C.; Dean, D. R. *J. Inorg. Biochem.* **2007**, *101*, 1642.
- (19) Sarma, R.; Barney, B. M.; Keable, S.; Dean, D. R.; Seefeldt, L. C.; Peters, J. W. *J. Inorg. Biochem.* **2010**, *104*, 385.
- (20) Yang, Z.-Y.; Dean, D. R.; Seefeldt, L. C. *J. Biol. Chem.* **2011**, *286*, 19417.
- (21) Benton, P. M. C.; Laryukhin, M.; Mayer, S. M.; Hoffman, B. M.; Dean, D. R.; Seefeldt, L. C. *Biochemistry* **2003**, *42*, 9102.
- (22) Lee, H.-I.; Igarashi, R.; Laryukhin, M.; Doan, P. E.; Dos Santos, P. C.; Dean, D. R.; Seefeldt, L. C.; Hoffman, B. M. *J. Am. Chem. Soc.* **2004**, *126*, 9563.
- (23) Igarashi, R.; Dos Santos, P. C.; Niehaus, W. G.; Dance, I. G.; Dean, D. R.; Seefeldt, L. C. *J. Biol. Chem.* **2004**, *279*, 34770.
- (24) Barney, B. M.; Laryukhin, M.; Igarashi, R. Y.; Lee, H.-I.; Dos Santos, P. C.; Yang, T.-C.; Hoffman, B. M.; Dean, D. R.; Seefeldt, L. C. *Biochemistry* **2005**, *44*, 8030.
- (25) Igarashi, R. Y.; Laryukhin, M.; Dos Santos, P. C.; Lee, H.-I.; Dean, D. R.; Seefeldt, L. C.; Hoffman, B. M. *J. Am. Chem. Soc.* **2005**, *127*, 6231.
- (26) Barney, B. M.; Lee, H.-I.; Dos Santos, P. C.; Hoffman, B. M.; Dean, D. R.; Seefeldt, L. C. *Dalton Trans.* **2006**, 2277.
- (27) Barney, B. M.; McClead, J.; Lukoyanov, D.; Laryukhin, M.; Yang, T. C.; Dean, D. R.; Hoffman, B. M.; Seefeldt, L. C. *Biochemistry* **2007**, *46*, 6784.
- (28) Barney, B. M.; Lukoyanov, D.; Igarashi, R. Y.; Laryukhin, M.; Yang, T.-C.; Dean, D. R.; Hoffman, B. M.; Seefeldt, L. C. *Biochemistry* **2009**, *48*, 9094.
- (29) Hoffman, B. M.; Dean, D. R.; Seefeldt, L. C. *Acc. Chem. Res.* **2009**, *42*, 609.
- (30) Doan, P. E.; Telser, J.; Barney, B. M.; Igarashi, R. Y.; Dean, D. R.; Seefeldt, L. C.; Hoffman, B. M. *J. Am. Chem. Soc.* **2011**, *133*, 17329.
- (31) Danyal, K.; Yang, Z.-Y.; Seefeldt, L. C. *Methods Mol. Biol.* **2011**, *766*, 191.
- (32) Lukoyanov, D.; Dikanov, S. A.; Yang, Z.-Y.; Barney, B. M.; Samoilova, R. I.; Narasimhulu, K. V.; Dean, D. R.; Seefeldt, L. C.; Hoffman, B. M. *J. Am. Chem. Soc.* **2011**, *133*, 11655.
- (33) Lukoyanov, D.; Yang, Z.-Y.; Barney, B. M.; Dean, D. R.; Seefeldt, L. C.; Hoffman, B. M. *Proc. Natl. Acad. Sci. U.S.A.* **2012**, *109*, 5583.
- (34) Yan, L.; Dapper, C. H.; George, S. J.; Wang, H.; Mitra, D.; Dong, W.; Newton, W. E.; Cramer, S. P. *Eur. J. Inorg. Chem.* **2011**, 2064.
- (35) Yang, Z.-Y.; Seefeldt, L. C.; Dean, D. R.; Cramer, S. P.; George, S. J. *Angew. Chem., Int. Ed.* **2011**, *50*, 272.
- (36) George, S. J.; Barney, B. M.; Mitra, D.; Igarashi, R. Y.; Guo, Y.; Dean, D. R.; Cramer, S. P.; Seefeldt, L. C. *J. Inorg. Biochem.* **2012**, *112*, 85.
- (37) Yan, L.; Pelmenschikov, V.; Dapper, C. H.; Scott, A. D.; Newton, W. E.; Cramer, S. P. *Chem.—Eur. J.* **2012**, *18*, 16349.
- (38) Durrant, M. C. *Biochem. J.* **2001**, *355*, 569.
- (39) Dance, I. *Dalton Trans.* **2012**, *41*, 7647.
- (40) Barney, B. M.; Yurth, M. G.; Dos Santos, P. C.; Dean, D. R.; Seefeldt, L. C. *J. Biol. Inorg. Chem.* **2009**, *14*, 1015.
- (41) Dance, I. *Sci. Rep.* **2013**, manuscript in preparation.
- (42) Dance, I. *J. Am. Chem. Soc.* **2005**, *127*, 10925.
- (43) Dance, I. *Biochemistry* **2006**, *45*, 6328.
- (44) Dance, I. *Dalton Trans.* **2008**, 5977.
- (45) Dance, I. *Dalton Trans.* **2008**, 5992.
- (46) Dance, I. *Dalton Trans.* **2011**, *40*, 5516.
- (47) Thorneley, R. N. F.; Lowe, D. J. In *Molybdenum Enzymes*; Spiro, T. G., Ed.; Wiley Interscience: New York, 1985; p 221.
- (48) Dance, I. *Chem.—Asian J.* **2007**, *2*, 936.
- (49) Dance, I. *J. Am. Chem. Soc.* **2007**, *129*, 1076.
- (50) Delley, B. *J. Chem. Phys.* **1990**, *92*, 508.
- (51) Delley, B. In *Modern Density Functional Theory: A Tool for Chemistry*; Seminario, J. M., Politzer, P., Eds.; Elsevier: Amsterdam, 1995; Vol. 2, p 221.
- (52) Delley, B. *J. Chem. Phys.* **2000**, *113*, 7756.
- (53) Dance, I. *Inorg. Chem.* **2006**, *45*, 5084.
- (54) Dance, I. *Dalton Trans.* **2012**, *41*, 4859.
- (55) Dance, I. *Inorg. Chem.* **2011**, *50*, 178.
- (56) Dance, I. *Mol. Simul.* **2008**, *34*, 923.
- (57) Dance, I. *Mol. Simul.* **2011**, *37*, 257.
- (58) Dance, I. **2013**, manuscript in preparation.
- (59) Nagel, Z. D.; Klinman, J. P. *Chem. Rev.* **2010**, *110*, PR41.
- (60) <http://www.ccdc.cam.ac.uk>, 2013.
- (61) Long, J. R.; McCarty, L. S.; Holm, R. H. *J. Am. Chem. Soc.* **1996**, *118*, 4603.
- (62) Qin, Y.-H.; Wu, M.-M.; Chen, Z.-N. *Acta Crystallogr., Sect. E* **2003**, *59*, m317.
- (63) Han, L.; Shi, L.-X.; Zhang, L.-Y.; Chen, Z.-N.; Hong, M.-C. *Inorg. Chem. Commun.* **2003**, *6*, 281.
- (64) Kuwata, S.; Hidai, M. *Coord. Chem. Rev.* **2001**, *213*, 211.